An integral equation approach to fracture propagation in rocks

N. J. ALTIERO *, G. GIODA **

SUMMARY: A seemingly novel integral equation approach is presented for the analysis of propagating fractures in plane regions. The crack is modelled by a continuous distribution of *Edge Dislocations*. Arbitrary distributions of both free field stresses and internal tractions on the crack surfaces are accounted for and the governing equations are derived assuming homogeneous, isotropic, elastic-brittle material behaviour. A fundamental feature of this approach is that only geometrical information describing the shape and the size of the fracture is necessary. This allows one to easily generate the additional geometrical data for the propagated portions of the crack with negligible effort. A simple technique for numerical solution is outlined, and the results obtained by analyzing a series of non-growing and propagating fractures are discussed.

1. Introduction

The propagation analysis of pressurized, or internally loaded, fractures is a problem of considerable importance in Rock Mechanics. It is well known, in fact, that the so called « hydraulic fracturing » [JAWORSKI *et al.*, 1981] may develop spontaneously in the core of dams, or in the underlying rock, and is believed to be a possible cause of collapse of some dams. In other cases, the same phenomenon can be artificially induced in order to determine the in situ stresses in deep rock formations.

Recently, the growing need for alternative sources of energy has brought to the attention of rock engineers a new area in which hydraulic fracturing has potential applicability: « extraction » of heat from deep, hot, dry rocks.

The technique envisaged for this purpose requires two vertical boreholes to be drilled to the desired depth. Then, two horizontal fractures are propagated from the bottom of the boreholes by applying a high pressure of fluid in their final portions. If the cracks meet at a point between the vertical holes, a U-shaped circuit is established with the surface. This allows one to pump cool water into one of the boreholes and to extract hot water or steam, to be used for electricity production, from the other.

In order for this procedure to be effective, it is essential to predict with reasonable accuracy the path of crack propagation on the basis of the in situ stress in the rock mass and of the applied internal pressure. The same type of analysis could be useful in designing dams against failure due to hydraulic fracturing.

Several numerical approaches have been presented in the literature for the study of propagating cracks. They are here grouped into three categories, without attempt to present an exhaustive classification, but merely with the intention of emphasizing the basic conceptual and operative differences between them.

a) A first possible approach [MURAKAMI, 1976; INGRAFFEA, HEUZE, 1980] is based on the *finite element* discretization of the medium surrounding the fracture. The crack coincides with the line of separation between some of the elements, hence, the nodes of the elements facing the two sides of it are not connected to each other. The stress concentration in the vicinity of the tip is approximated either by adopting a very fine mesh close to the crack end or by introducing « singular » elements in this position. The approach is particularly effective for determining stress fields and stress intensity factors for non-growing cracks. However, it requires cumbersome modifications of the mesh (and apparently prohibitive computational and programming efforts) if the fractures propagate in *a priori* unknown, and continuously changing, directions.

b) A second procedure based on the finite element method considers the fracture as a band of parallel cracks smeared over the entire finite element [BAZANT, CEDOLIN, 1979; CEDOLIN, BAZANT, 1980]. This approach can be considered somewhat similar to the analysis of spreading of « plastic » zones having particular mechanical characteristics. The procedure offers considerable advantages with respect to those

* Nicholas J. ALTIERO, Associate Professor, Department of *Metallurgy, Mechanics and Material Science*, Michigan State University, East Lansing, U.S.A.

** Giancarlo GIODA, Associate Professor, Department of *Structural Engineering*, Technical University (Politecnico) of Milan, Italy.

of group (a), especially because it does not require modifications of the mesh as the crack propagates, and it appears particularly effective for problems where several close cracks develop simultaneously in a limited area, e.g. in reinforced concrete structural members. However, its application to the propagation of a single pressurized crack appears less promising, mainly because of the indetermination of the exact position of the propagated part of the fracture.

c) The third technique is based on the *boundary integral* method [MIR-MOHAMAD - SADEGH, ALTIERO, 1979; MURAKAMI, 1980; BLANDFORD *et al.*, 1981]. Various approaches of the *direct* and *indirect* types have been presented in the literature, and discussion of them falls outside the limits of the present work. It can be observed, however, that some of these approaches consider the influence of a crack of given shape already embodied in the fundamental equations governing the problem and, hence, do not appear suitable for propagation analyses which involve variation of the crack geometry. The approaches applicable to propagation analyses usually subdivide the body containing the fracture into two regions by means of an artificial boundary, a portion of which coincides with the initial crack. After subdivision, the two regions are connected along the common boundary but for the cracked portion. Singular « boundary elements », or very fine subdivision of the boundary, can be adopted at the fracture tips. Obviously this method requires less geometrical data than those of group (a). On the other hand, a complete description of the geometry of the artificial boundary (which exceed the cracked zone) is required. As a consequence, for propagation analyses, it is necessary to modify the geometrical data of the crack and also of the zones of the boundary ahead and behind it. This introduces problems basically similar to those mentioned for the approaches of group (a).

Note also that these methods cannot be directly applied to the propagation of cracks in unbounded regions. This drawback is overcome by discretizing only a part (usually large) of the medium, and neglecting the induced boundary effects, at the expense of a remarkable increase in the number of free variables.

In this paper a boundary integral approach is presented for the propagation analysis of fracture of negligible thickness, situated in an infinite plane region and modelled by a continuous distribution of *edge dislocations*. Generic distributions of both free field stresses and internal tractions on the crack contour are accounted for. The same approach, coupled with other classical boundary integral procedures for stress analysis, is applicable to the study of fractures in finite domains.

The problem is treated in plane strain, or plane stress, assuming homogeneous, isotropic, linear elastic-brittle material behaviour.

A basic characteristic of the approach is that geometrical data are required only for describing the shape and the size of the crack. This considerably reduces the amount of necessary geometrical information, with respect to other approaches, and makes it possible the automatic generation of these data for propagating fractures with negligible computational and programming efforts.

In the following, the equations governing the problem are first presented. Then, a simple procedure for numerical solution is outlined, based on the piecewise linear discretization of the crack and on the *strain energy density criterion* for fracture propagation. Finally, the results of a series of applications are discussed. These concern the determination of stress distribution and stress intensity factors for non-growing cracks, and the prediction of the paths of growth for propagating cracks.

2. Boundary integral approach

Consider a crack of length L in a homogeneous, isotropic, linear elastic, infinite plane region and suppose that the crack surfaces are subjected to normal $p_n(s)$ and tangential $p_t(s)$ traction distributions, s being the curvilinear abscissa along the crack, as shown in fig. 1. If the crack is modelled by a continuous distribution of *Edge Dislocations* [READ, 1953] with components $C_n(s)$ and $C_t(s)$, the tractions $p_n(s)$ and $p_t(s)$ can be expressed by the following superpositions:

$$\int_0^L [I_{nn}(s,\bar{s}) \cdot C_n(\bar{s}) + I_{nt}(s,\bar{s}) \cdot C_t(\bar{s})] \, d\bar{s} = p_n(s) \qquad (1a)$$

$$\int_0^L [I_{tn}(s,\bar{s}) \cdot C_n(\bar{s}) + I_{tt}(s,\bar{s}) \cdot C_t(\bar{s})]\, d\bar{s} = p_t(s) \tag{1b}$$

In the above integrals, wich are to be interpreted in the Cauchy principle value sense, the influence function $I_{ij}(s,\bar{s})$ represents the i-th component of the stress vector at s due to a unit j-th component of a dislocation vector applied at $\bar{s}$.

Assuming that the region surrounding the crack is in plane stress conditions, the influence functions are expressed by the following relationships:

$$I_{nn} = \frac{G(1+\nu)}{2\pi\rho}[k_8 q_x - k_3 q_y + 2 k_1 q^3_x - 2 k_2 q^3_y] \tag{2a}$$

$$I_{nt} = \frac{G(1+\nu)}{2\pi\rho}[k_7 q_x + k_4 q_y - 2 k_2 q^3_x - 2 k_1 q^3_y] \tag{2b}$$

$$I_{tn} = \frac{G(1+\nu)}{2\pi\rho}[k_6 q_x + k_5 q_y - 2 k_2 q^3_x - 2 k_1 q^3_y] \tag{2c}$$

$$I_{tt} = \frac{G(1+\nu)}{2\pi\rho}[k_5 q_x - k_6 q_y - 2 k_1 q^3_x + 2 k_2 q^3_y] \tag{2d}$$

where G is the shear modulus, ν is Poisson's ratio,

$$q_x = \frac{x - \bar{x}}{\rho}\ ;\ q_y = \frac{y - \bar{y}}{\rho}\ ;\ \rho = [(x-\bar{x})^2 + (y-\bar{y})^2]^{1/2} \tag{3a, b, c}$$

and

$$k_1 = 2 n_x n_y \bar{n}_x + (n^2_x - n^2_y)\bar{n}_y\ ;\ k_2 = 2 n_x n_y \bar{n}_y - (n^2_x - n^2_y)\bar{n}_x \tag{4a, b}$$

$$k_3 = 2 n^2_x \bar{n}_x - k_2\ ;\ k_4 = 2 n^2_x \bar{n}_y + k_1\ ;\ k_5 = 2 n_x n_y \bar{n}_x + k_1 \tag{4c, d, e}$$

$$k_6 = 2 n_x n_y \bar{n}_y + k_2\ ;\ k_7 = 2 n^2_y \bar{n}_x + k_2\ ;\ k_8 = 2 n^2_y \bar{n}_y - k_1 \tag{4f, g, h}$$

In eqs. (4), n_x and n_y are the direction cosines of the unit vector normal to the crack contour (cfr. fig. 1).

Eqs. (2) hold also for plane strain conditions if ν is replaced, as customary, with an « equivalent » Poisson's ratio ν' defined as

$$\nu' = \nu/(1-\nu) \tag{5}$$

Substitution of eqs. (2) into eqs. (1) yields

$$\int_0^L \frac{1}{\rho}[(k_8 q_x - k_3 q_y + 2k_1 q^3_x - 2k_2 q^3_y) \cdot C_n + (k_7 q_x + k_4 q_y - 2k_2 q^3_x - 2k_1 q^3_y) \cdot C_t]\, d\bar{s} = \tag{6a}$$

$$= \frac{2\pi}{G(1+\nu)} \cdot p_n(s)$$

$$\int_0^L \frac{1}{\rho}\,[(k_6\,q_x + k_5\,q_y - 2k_2\,q^3_x - 2k_1\,q^3_y)\cdot C_n + (k_5\,q_x - k_6\,q_y - 2k_1\,q^3_x + 2k_2\,q^3_y)\cdot C_t]\,d\bar{s} = \frac{2\pi}{G(1+\nu)}\cdot p_t(s) \tag{6b}$$

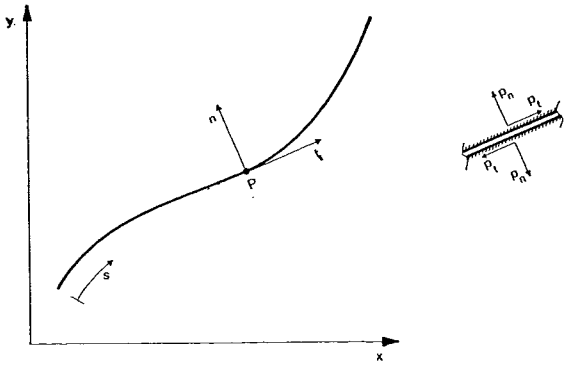

Fig. 1. - Notation adopted in the boundary integral formulation of the continuous problem.

Fig. 1. - Notazione adottata nella formulazione del problema continuo.

Therefore, if $p_n(s)$ and $p_t(s)$ are known functions, eqs. (6) represent a coupled set of integral equations to be solved for $C_n(s)$ and $C_t(s)$. Note that the edge dislocation functions, as defined here, represent jumps in the components of the distortion vector as the crack contour is crossed in the direction of n. Thus, at a point $s = s_o$ close to the crack tip, assuming the part of the fracture from $s = 0$ to $s = s_o$ as a straight segment, one can write

$$\Delta u_n(s_o) = \int_0^{s_o} C_n(\bar{s})\; d\bar{s}\;;\quad \Delta u_t(s_o) = \int_0^{s_o} C_t(\bar{s})\; d\bar{s} \tag{7a, b}$$

where Δu_n and Δu_t are the jumps in the normal and tangential displacements, respectively, of the crack surfaces.

The stresses σ_{ij} and the displacements u_i in the medium surrounding the crack can be computed, once the distribution of edge dislocations has been determined, by means of the following integrals

$$\sigma_{ij} = \int_0^L [I^{\sigma}_{ij,n}\cdot C_n + I^{\sigma}_{ij,t}\cdot C_t]\,d\bar{s}\;;\quad u_i = \int_0^L [I^{u}_{i,n}\cdot C_n + I^{u}_{i,t}\cdot C_t]\,d\bar{s} \tag{8a, b}$$

$(i,j = x,y)$ $\qquad$ $(i = x,y)$

where the influence functions I^{σ} and I^{u} can be expressed in the following compact forms

$$\begin{Bmatrix} I^{\sigma}_{xx,n} \\ I^{\sigma}_{xx,t} \\ I^{\sigma}_{xy,n} \\ I^{\sigma}_{xy,t} \\ I^{\sigma}_{yy,n} \\ I^{\sigma}_{yy,t} \end{Bmatrix} = \frac{G(1+\nu)}{2\pi} \begin{bmatrix} 0 & 1 & -3 & 0 & 0 & -1 & -1 & 0 \\ 1 & 0 & 0 & 3 & -1 & 0 & 0 & 1 \\ 1 & 0 & 0 & 1 & -1 & 0 & 0 & -1 \\ 0 & -1 & 1 & 0 & 0 & 1 & -1 & 0 \\ 0 & 1 & 1 & 0 & 0 & 3 & -1 & 0 \\ 1 & 0 & 0 & -1 & 3 & 0 & 0 & 1 \end{bmatrix} \begin{Bmatrix} \bar{n}_x\,q^3_x/\rho \\ \bar{n}_y\,q^3_x/\rho \\ \bar{n}_x\,q^2_x\,q_y/\rho \\ \bar{n}_y\,q^2_x\,q_y/\rho \\ \bar{n}_x\,q_x\,q^2_y/\rho \\ \bar{n}_y\,q_x\,q^2_y/\rho \\ \bar{n}_x\,q^3_y/\rho \\ \bar{n}_y\,q^3_y/\rho \end{Bmatrix} \tag{9a}$$

$$\begin{Bmatrix} I^{u}_{x,n} \\ I^{u}_{x,t} \\ I^{u}_{y,n} \\ I^{u}_{y,t} \end{Bmatrix} = \frac{1}{4\pi} \begin{bmatrix} 0 & -a & 0 & -b & b & 0 & 0 & 0 & 2 & 0 \\ -a & 0 & -b & 0 & 0 & -b & 0 & 0 & 0 & -2 \\ a & 0 & 0 & 0 & 0 & -b & b & 0 & 0 & 2 \\ 0 & -a & 0 & 0 & -b & 0 & 0 & -b & 2 & 0 \end{bmatrix} \begin{Bmatrix} \bar{n}_x\,\ln\rho \\ \bar{n}_y\,\ln\rho \\ \bar{n}_x\,q^2_x \\ \bar{n}_y\,q^2_x \\ \bar{n}_x\,q_x\,q_y \\ \bar{n}_y\,q_x\,q_y \\ \bar{n}_x\,q^2_y \\ \bar{n}_y\,q^2_y \\ \bar{n}_x\,\tan^{-1}\Phi \\ \bar{n}_y\,\tan^{-1}\Phi \end{Bmatrix} \tag{9b}$$

The expressions of coefficients a, b and Φ in eqs. (9) are

$$a = \nu - 1 \; ; \; b = \nu + 1 \; ; \; \Phi = \frac{q_y \bar{n}_x - q_x \bar{n}_y}{q_x \bar{n}_x + q_y \bar{n}_y} \qquad (10a, b, c)$$

and q_x, q_y and ρ are defined by eqs. (3). Note that in these expressions the dashed variables refer to the point on the crack while x and y are the co-ordinates of the field point where stresses and displacements are sought.

A relation between the edge dislocation distribution and the modes I and II stress intensity factors, K_I and K_{II}, can be established considering that the following equation hold if s_o is chosen sufficiently small

$$\Delta u_n(s_o) = K_I \Big|_{s=o} \cdot \frac{4\sqrt{s_o}}{G(1+\nu)\sqrt{2\pi}} \; ; \; \Delta u_t(s_o) = K_{II} \Big|_{s=o} \cdot \frac{4\sqrt{s_o}}{G(1+\nu)\sqrt{2\pi}} \qquad (11a, b)$$

Equating the displacement discontinuities given by eqs. (7) and (11), the following expressions of the stress intensity factors are arrived at

$$K_I \Big|_{s=o} = \frac{G(1+\nu)\sqrt{2\pi}}{4\sqrt{s_o}} \int_o^{s_o} C_n(\bar{s})\, d\bar{s} \qquad (12a)$$

$$K_{II} \Big|_{s=o} = \frac{G(1+\nu)\sqrt{2\pi}}{4\sqrt{s_o}} \int_o^{s_o} C_t(\bar{s})\, d\bar{s} \qquad (12b)$$

The above equations, and the equivalent ones for s = L, allows one to obtain the stress intensity factors at the two tips of the crack, once the distribution of edge dislocations has been determined by solving eqs. (6).

In order to compare the solution obtained by the described approach with the exact one, for a simple « bench mark » problem, consider a straight crack of lenght L subjected to a constant distribution of internal normal tractions. For this case the following simplifying relations hold

$$\bar{n}_x = n_x \; ; \; \bar{n}_y = n_y \; ; \; q^2_x = n^2_y \; ; \; q^2_y = n^2_x \qquad (13a, b, c, d)$$

$$\frac{q_x}{\rho} = \frac{n_y}{s - \bar{s}} \; ; \; \frac{q_y}{\rho} = -\frac{n_x}{s - \bar{s}} \qquad (13e, f)$$

and eq. (6a) reduces to

$$\int_o^L \frac{C_n(\bar{s})}{s - \bar{s}}\, d\bar{s} = \frac{2\pi}{G(1+\nu)} \cdot p_n \qquad (14)$$

It can be shown that the solution of eq. (14) for constant p_n is

$$C_n(s) = \frac{1}{G(1+\nu)} \left[\frac{\sqrt{L - s}}{\sqrt{s}} - \frac{\sqrt{s}}{\sqrt{L - s}} \right] p_n \qquad (15)$$

which, for $s << L$, can be re-written in the form

$$C_n(s) = \frac{1}{G(1+\nu)} \frac{\sqrt{L}}{\sqrt{s}} p_n \qquad (16)$$

Substitution of eq. (16) into eq. (12a) leads to the following expression for K_I

$$K_I\Big|_{s=o} = p_n \frac{\sqrt{2\pi L}}{4\sqrt{s_o}} \int_o^{s_o} \frac{d\bar{s}}{\sqrt{\bar{s}}} \qquad (17a)$$

and hence

$$K_I\Big|_{s=o} = p_n \sqrt{\pi L/2} \qquad (17b)$$

The expression of K_I given in eq. (17b) coincides with the exact one. An analogous derivation leads to the mode II stress intensity factor for a straight crack subjected to an uniform shear distribution along its contour, which again is equal to the exact one.

It is worth mentioning that the described approach is not confined to the analysis of pressurized, or internally loaded, cracks only. In fact, the stress distribution in the neighborhood of an unloaded crack in a plane region under known free field stresses (cfr. fig. 2a), can be obtained by simply superposing the stress distribution in the uncracked region (fig. 2b) with the one due to surface tractions on the crack equal in modulus and opposite in sign to the free field stresses (fig. 2c). Obviously, for cracks of general shape and/or for generic distribution of free field stresses, the problem schematically shown in fig. 2c will involve both normal and tangential non uniform traction distributions along the crack.

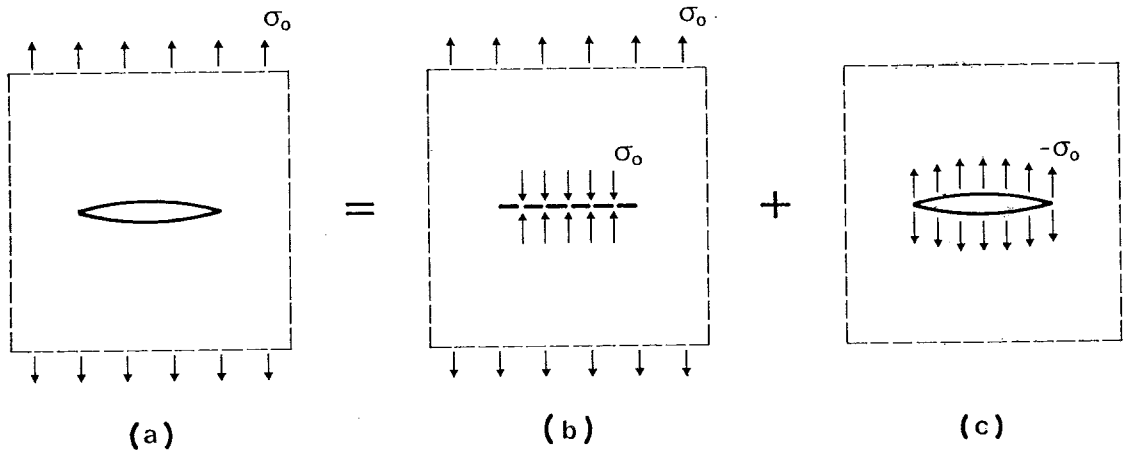

Fig. 2. - Solution for an internally unloaded crack as superposition of two problems,

Fig. 2. - Rappresentazione di una frattura non soggetta a pressione interna tramite sovrapposizione degli effetti.

3. A simple numerical treatment

In order to assess the capability of the proposed approach to analyse crack propagation problems, a numerical procedure was implemented for the solution of the integral equations (6) based on the piecewise linear discretization of the crack, as shown in fig. 3. The edge dislocations C_n and C_t are assumed constant along each crack segment and equal to their value at the segment mid-point. Under these assumptions, eqs. (6) can be re-written in the following form for the i-th mid-point (or segment)

$$\sum_{\substack{j=1 \\ (j \neq i)}}^{N} \left\{ C_n^{(j)} \left[\int_{s_{j-1}}^{s_j} \frac{1}{\rho} (k_8 q_x - k_3 q_y + 2k_1 q^3_x - 2k_2 q^3_y)\, d\bar{s} + \right. \right.$$

$$\left. \left. + C_t^{(j)} \left[\int_{s_{j-1}}^{s_j} \frac{1}{\rho} (k_7 q_x + k_4 q_y - 2k_2 q^3_x - 2k_1 q^3_y) d\bar{s} \right] \right\} = \frac{2\pi}{G(1+\nu)} p_n^{(i)} \qquad (18a)$$

$$\sum_{\substack{j=1\\(j\neq i)}}^{N}\left\{C_n^{(j)}\left[\int_{s_{j-1}}^{s_j}\frac{1}{\rho}(k_6\,q_x+k_5\,q_y-2k_2\,q^3{}_x-2k_1\,q^3{}_y)\;d\bar{s}\right]+\right.$$

$$\left.+\,C_t^{(j)}\left[\int_{s_{j-1}}^{s_j}\frac{1}{\rho}(k_5\,q_x-k_6\,q_y-2k_1\,q^3{}_x+2k_2\,q^3{}_y)\;d\bar{s}\right]\right\}=\frac{2\pi}{G(1+\nu)}\,p_t^{(i)} \tag{18b}$$

where N is the number of subdivisions and the expressions for ρ, q_x, q_y and for the coefficients k are obtained from eqs. (3) and (4) by replacing x, y with x_i, y_i and $\bar{x}$, $\bar{y}$ with x_j, y_j (cfr. fig. 3).

If eqs. (18) are written for all the segments of the piecewise linearized crack (which is equivalent to satisfy the loading conditions at the mid-point of each segment), a system of 2N linear equations is obtained for the 2N unknowns $C_n^{(j)}$, $C_t^{(j)}$ (j = 1, N). It can be shown that writing eq. (6) in the discretized form for i = j, the coefficients multiplying $C_n^{(i)}$ and $C_t^{(i)}$ vanish. This means in turn that all the terms of the main diagonal of the assembled system matrix vanish.

As for the majority of the boundary integral approaches, the matrix of coefficients is in general fully populated and non symmetric.

Having determined the distribution of edge dislocations, the values of the mode I and II stress intensity factors for the first crack tip (s = o) can be determined by means of eqs. (12),

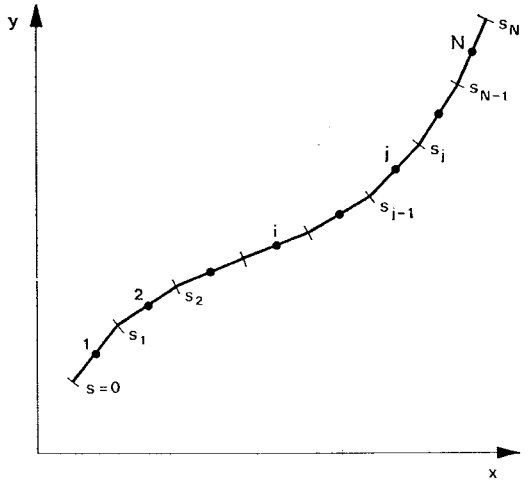

Fig. 3 - Notation for the discretized problem.

Fig. 3. - Notazione adottata nella formulazione del problema discretizzato.

which for the discretized problem, assuming $s_o = s_2$, read

$$K_I\Big|_{s=o}=\frac{G(1+\nu)\sqrt{2\pi}}{4\sqrt{s_2}}\left[C_n^{(1)}\,s_1+C_n^{(2)}\,(s_2-s_1)\right] \tag{19a}$$

$$K_{II}\Big|_{s=o}=\frac{G(1+\nu)\sqrt{2\pi}}{4\sqrt{s_2}}\left[C_t^{(1)}\,s_1+C_t^{(2)}\,(s_2-s_1)\right] \tag{19b}$$

Similar equations define the values of the stress intensity factors for the second tip of the crack (s = L). Obviously, an accurate determination of K_I and K_{II} requires a careful choice of the lenght of the segments close to the crack tips.

The determination of the direction in which the crack propagates under mixed mode conditions has been based here on the *Strain Energy Density Criterion* proposed by SIH [1973].

In the vicinity of the crack tip (cfr. fig. 4)

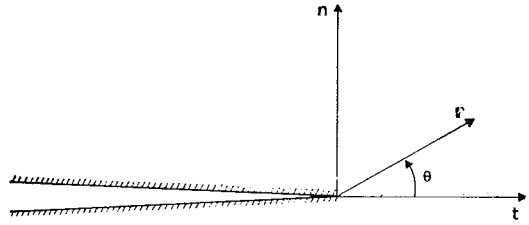

Fig. 4 - Co-ordinate system at the crack tip for the Strain Energy Density Criterion for fracture propagation.

Fig. 4. - Sistema di coordinate radiali adottato nell'espressione del criterio di propagazione della frattura.

the strain energy density can be expressed by the following relationship

$$\frac{dW}{dV} = \frac{1}{r} S(\theta) + \text{non-singular terms} = \frac{1}{r} (c_{11} K_I^2 + 2c_{12} K_I K_{II} + c_{22} K_{II}^2) + \ldots \quad (20)$$

where W is the strain energy, V in the volume and the coefficients c_{ij} for plane problems are

$$c_{11} = \frac{1}{16\pi G} [(1 + \cos\theta)(\varkappa - \cos\theta)] \quad (21a)$$

$$c_{12} = \frac{\sin\theta}{16\pi G} [2\cos\theta - (\varkappa - 1)] \quad (21b)$$

$$c_{22} = \frac{1}{16\pi G} [(\varkappa + 1)(1 - \cos\theta) + (1 + \cos\theta)(3\cos\theta - 1)] \quad (21c)$$

$$\varkappa = (3 - \nu)/(1 + \nu) \text{ plane stress} ; \varkappa = 4 - 3\nu \text{ plane strain} \quad (21d, e)$$

The criterion assumes that the crack propagates when the strain energy density factor S reaches a critical value S_c, which is a material property, and that the direction of propagation is defined by the minimum value of S, i.e.

$$\frac{dS}{d\theta} = 0 \quad \text{and} \quad \frac{d^2S}{d\theta^2} > 0 \quad (22a, b)$$

Note that the classical criterion for fracture propagation based on the critical value of the J-integral [RICE, 1968] cannot be adopted for the problem at hand. In fact, the fundamental property that makes the J-integral useful for practical applications is its paths independency, that can be proved only for cracks not subjected to internal tractions. As a consequence, this criterion appears to be not suitable for propagation analyses of pressurized cracks.

Once the direction of propagation is determined, the crack can be extended in that direction by simply adding a few segments to the already existing ones. Then a new analysis can be performed for the next propagation step.

It is important to note that the discussed boundary integral approach requires a very limited amount of geometrical data. In fact, all the geometrical quantities necessary in the analysis can be derived from the coordinates of the end points of the segments discretizing the fracture. As a consequence, the calculations required for defining the new geometry after a propagation increment are reduced to a minimum, and can be implemented in a small subroutine with negligible programming effort.

4. Illustrative applications

Two series of analyses were performed for the purpose of this study. The first one (the results of which are summarized in figs. 5 to 9) intends to provide some comparisons between

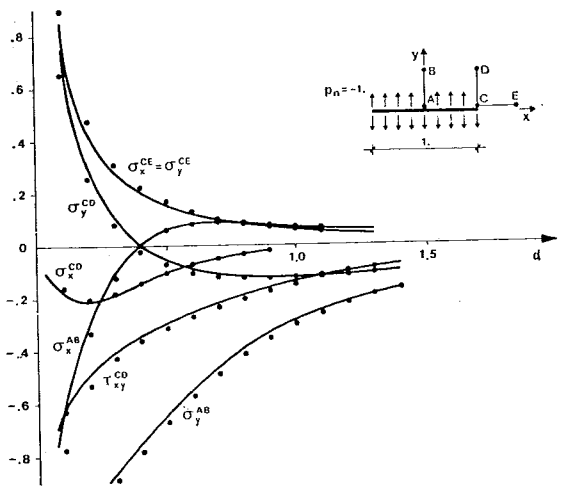

Fig. 5. - Stress distributions in the vicinity of a straight crack subjected to uniform internal pressure p_n. Analytical solution (solid lines) and boundary integral results (dots) with 40 fracture subdivisions.

Fig. 5. - Distribuzione degli sforzi attorno ad una frattura rettilinea soggetta a pressione interna p_n. Soluzione analitica (linee continue) e soluzione tramite gli integrali di contorno (punti) ottenuta con 40 suddivisioni della frattura.

the numerical solutions obtained with the proposed approach (in terms of stress distribution, values of the stress intensity factors and angles of initial propagation) and those, either analytical or numerical, presented in the literature for the same problems. The second series of analyses (figs. 10 to 14) concerns the determination of the propagation path of initially straight cracks under various loading conditions.

The problems have been solved in plane conditions assuming $G = 1$ and $\nu = 0.5$. For some of them the solution for $\nu = 0.0$ is also presented.

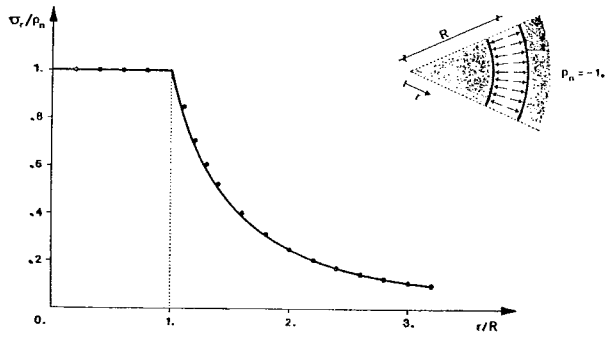

Fig. 6. - Radial stress distribution in the vicinity of a circular crack subjected to uniform internal pressure p_n. Analytical solution (solid lines) and boundary integral results (dots) with 72 fracture subdivisions.

Fig. 6. - Distribuzione dello sforzo radiale nelle vicinanze di una frattura circolare soggetta a pressione interna p_n. Soluzione analitica (linea continua) e soluzione tramite gli integrali di contorno (punti) ottenuta con 72 suddivisioni della frattura.

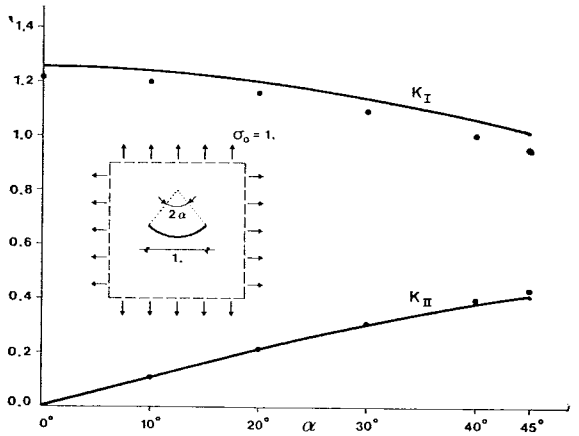

Fig. 7. - Stress intensity factors K_I and K_{II} for a circular arc crack under hydrostatic tensile stress σ_0 at infinity. Analytical solution [MUSKHELISHVILI, 1953; COTTEREL, RICE, 1980] (solid lines) and boundary integral results (dots) with 40 fracture subdivisions.

Fig. 7. - Fattori di concentrazione degli sforzi K_I e K_{II} per una frattura a forma di arco circolare soggetta ad uno stato uniforme di trazione σ_0 all'infinito. Soluzione analitica [MUSKHELISHVILI, 1953], [COTTEREL, RICE, 1980] *(linee continue) e soluzione tramite gli integrati di contorno (punti) ottenuta con 40 suddivisioni della frattura.*

Figs. 5 and 6 report the stress distribution in the vicinity of a straight crack and of a circular crack, both subjected to unit internal pressure. Solid lines represent the well known analytical solutions, while dots represent the numerical results obtained by subdividing the cracks into a number of segments (40 for the straight crack and 72 for the circular one) of constant lenght.

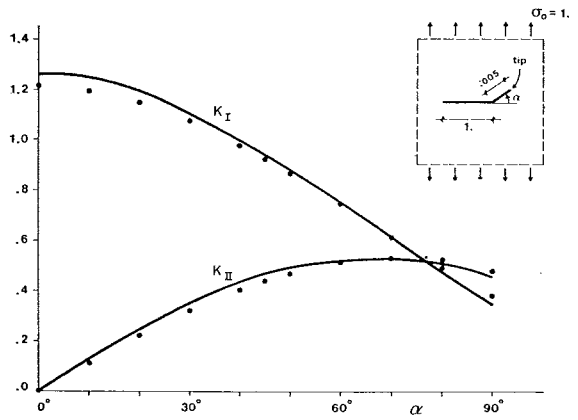

Fig. 8. - Stress intensity factors K_I and K_{II} at the kinked tip of a crack for uniform tensile stress σ_0 perpendicular to the main crack at infinity. Numerical solution [CHATTERJEE, 1975] (solid lines) and boundary integral results (dots) with 54 fracture subdivisions.

Fig. 8. - Fattori di concentrazione degli sforzi K_I e K_{II} per una frattura contenente un « gomito » soggetta a trazione σ_0 all'infinito in direzione normale alla porzione principale della frattura stessa. Soluzione numerica [CHATTERJEE, 1975] *(linee continue) e soluzione tramite gli integrali di contorno (punti) ottenuta con 54 suddivisioni della frattura.*

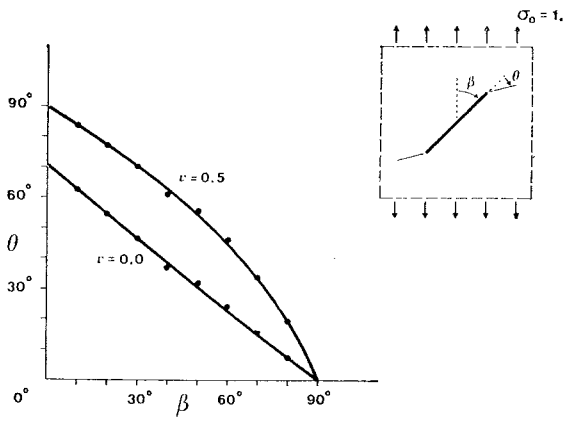

Fig. 9. - Angles of initial propagation of inclined straight cracks for uniform tensile stress σ_0 in the y direction at infinity. Analytical solution [SIH, 1973] (solid lines) and boundary integral results (dots) with 36 fracture subdivisions (plane strain conditions).

Fig. 9. - Angoli di propagazione di fratture inclinate ed inizialmente rettilinee soggette a sforzo di trazione σ_0 in direzione y all'infinito. Soluzione analitica [SIH, 1973] *(linee continue) e soluzione tramite gli integrali di contorno (punti) ottenuta in regime di deformazioni piane e con 36 suddivisioni della frattura.*

Some difference can be observed between numerical and analytical results approaching the tip of the straight crack. This is due to the low accuracy with which the stress concentration at the crack tip is determined by using relatively large subdivisions close to the tip. In order to avoid this effect, which is likely to have a remarkable influence on the determination of the stress intensity factors, the subsequent analyses have been performed adopting subdivisions with decreasing lenght approaching the crack tips. In particular, it was observed that a reasonable approximation can be achieved if the lenght of the segments close to the tips is about 0.001 the crack lenght.

Note that the problem of the circular crack provides, at the same time, the solution for a circular disk and for a circular hole in an infinite plane, both subjected to the same pressure distribution.

In figs. 7 and 8, the stress intensity factors K_I and K_{II} are shown for various shapes of a circular arc crack, for hydrostatic tensile stresses at infinity, and of a kinked crack, for tensile stresses normal to the main crack at infinity. The first set of numerical results is compared with the analytical solution derived by MUSKHELISHVILI [1953] and reported by COTTEREL, RICE [1980]; the second one is compared with a numerical solution, presented by CHATTERJEE [1975], developed *ad hoc* for kinked cracks.

It has to be pointed out that the simple numerical procedure here employed gives solutions of low accuracy when a sharp kink, greater that about 20°, is introduced in the discretization. This effect was eliminated by smoothing the kink with a small circular arc, so as to reduce the angle between two adjacent subdivisions below the mentioned limit.

Before solving crack propagation problems it is desirable to check the agreement between the angles of initial propagation predicted by the boundary integral technique and the analytical ones, for the same problem with the same propagation criterion. To this purpose, the angle of initial propagation of inclined straight cracks subjected to uniaxial tensile stresses at infinity were calculated and compared (cfr. fig. 9) to the analytical solution [SIH, 1973] based on the strain energy density criterion for fracture growth, with satisfactory agreement.

The results shown so far indicate that the proposed approach is capable to solve (with sufficient accuracy from the engineering view point) problems involving curved and kinked cracks (the later by introducing the mentioned « smoothing ») and that it can also predict angles of initial propagation consistent with the exact (analytical) ones. On this basis it seems reasonable to conclude that the approach could also handle cracks of general shape, and propagating cracks, which consist of curved and kinked portions.

The results of propagation analyses are presented in figs. 10 to 14, referring to initially straight fractures subjected to given stresses at infinity and/or to internal shear and normal tractions. For all the cases considered the propagation under constant loads is unstable. This means that the value of the strain energy density factor S (cfr. eq. 20), in the direction of growth, for the first increment is larger than those for the subsequent increments. Thus, propagation can be arrested only by reducing the values of the applied boundary and internal loads.

In fig. 10 the propagation paths are shown of two inclined cracks subjected to uniform uniaxial tensile stress at infinity for two values, 0.0 and 0.5, of Poisson's ratio. The calculations have been initially performed assuming $\Delta = 0.01L$ (Δ being the length of the increments and L the lenght of the crack before propagation) and subdividing each increment into 10 segments of constant lenght. Then, the same problems were solved reducing Δ to 0.005L, but keeping constant the number of segments per increment.

It turns out that the propagation paths for $\nu = 0.5$ have a relatively large radius of curvature and are practically independent from Δ. On the other hand, the radius of curvature decreases when $\nu = 0.0$ and two different solutions are obtained for $\Delta = 0.01L$ (solid lines in fig. 10) and for $\Delta = 0.005L$ (dashed lines). This indicates that appreciable errors in the numerical solution can be avoided only if the size of the increments does not exceed a limit value, which evidently depend on the (*a priori* unknown) radius of curvature of the propagated crack. No attempt was made to develop a specific criterion for determining this limiting value. However, a practical (even though costly) way to find it is to perform several analyses of the same problem, decreasing the value of the fracture increments, until the propagation path becomes independent on the increment size.

Figs. 11 and 12 show the propagation paths of an inclined crack under constant uniaxial tensile stress at infinity and for various values

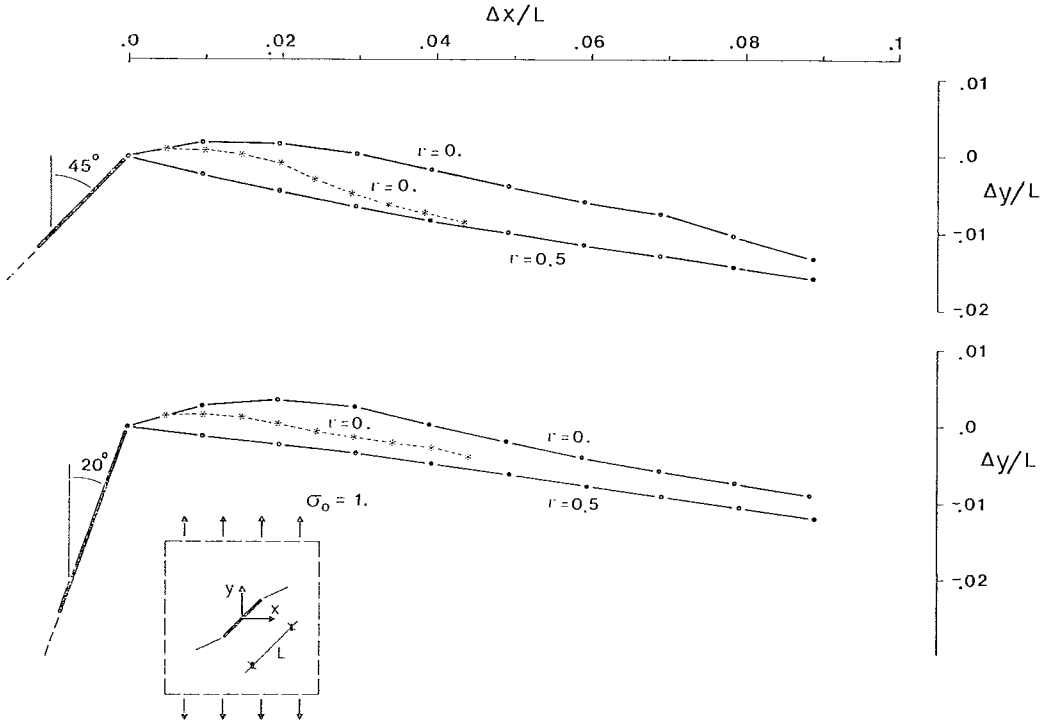

Fig. 10. - Propagation paths of inclined straight cracks for uniform tensile stress σ_0 in the y direction at infinity. Initial crack of lenght L subdivided into 36 segments. Fracture propagation increment equal to 0.01L (solid lines) and to 0.005L (dashed lines). Each increment divided into 10 segments (plane strain conditions).

Fig. 10. - Percorsi di propagazione di fratture inclinate ed inizialmente rettilinee soggette a sforzo di trazione σ_0 in direzione y *all'infinito. Frattura iniziale di lunghezza L suddivisa in 36 segmenti. Incremento di propagazione* Δ *eguale a 0.01L (linee continue) e a 0.005L (linee tratteggiate). Ogni incremento suddiviso in 10 segmenti. Stato piano nelle deformazioni.*

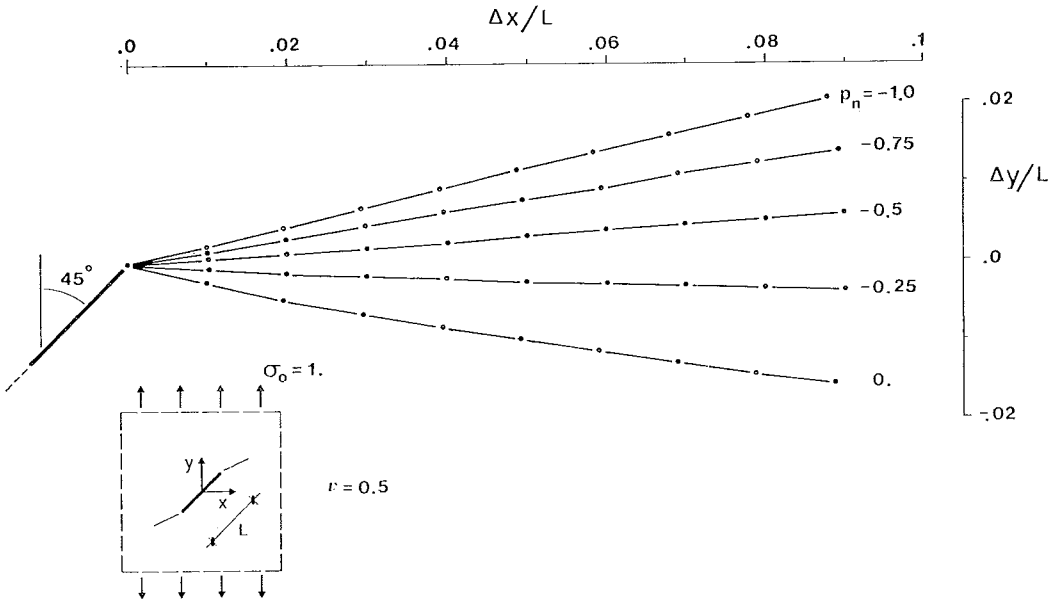

Fig. 11. - Propagation paths of an inclined straight crack for uniform tensile stress σ_0 in the y direction at infinity and uniform internal pressure p_n. Other characteristics as in fig. 10.

Fig. 11. - Percorsi di propagazione di una frattura inclinata ed inizialmente rettilinea soggetta a sforzo di trazione σ_0 in direzione y *all'infinito e a pressione interna* p_n. *Altre caratteristiche come in Fig. 10.*

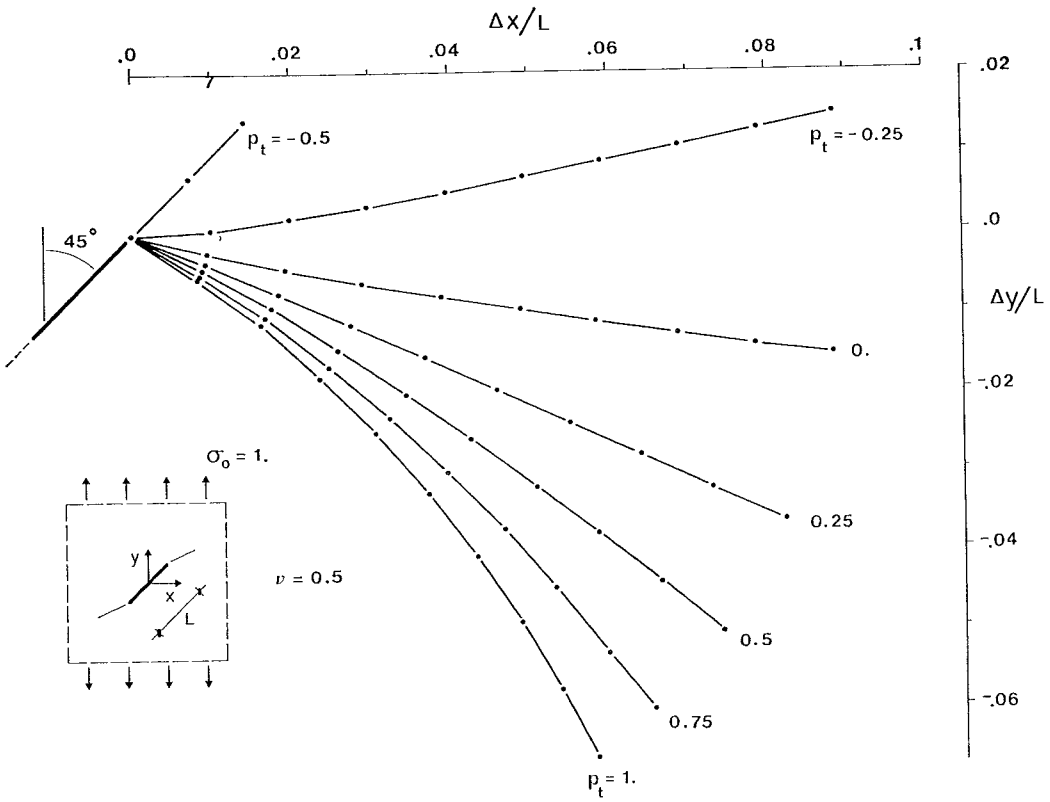

Fig. 12. - Propagation paths of an inclined straight crack for uniform tensile stress σ_0 in the y direction at infinity and uniform internal shear traction p_t. Other characteristics as in fig. 10.

Fig. 12. - Percorsi di propagazione di una frattura inclinata ed inizialmente rettilinea soggetta a sforzo di trazione σ_0 in direzione y *all'infinito e ad una distribuzione uniforme di sforzo tagliante p_t al suo interno. Altre caratteristiche come in Fig. 10.*

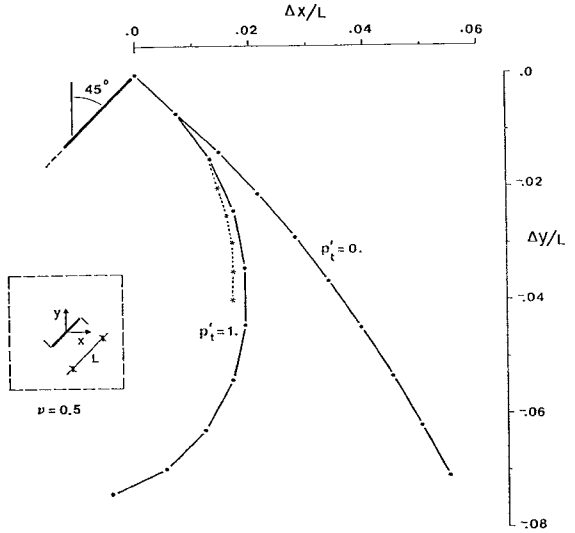

Fig. 13. - Propagation paths of a straight crack for uniform shear traction $p_t = 1$ on the initial crack and p'_t on the propagated portion. Other characteristics as in fig. 10.

Fig. 13. - Percorsi di propagazione di una frattura inizialmente rettilinea soggetta ad una distribuzione di sforzo tagliante $p_t = 1$ all'interno della frattura iniziale e p'_t all'interno della parte propagata. Altre caratteristiche come in Fig. 10.

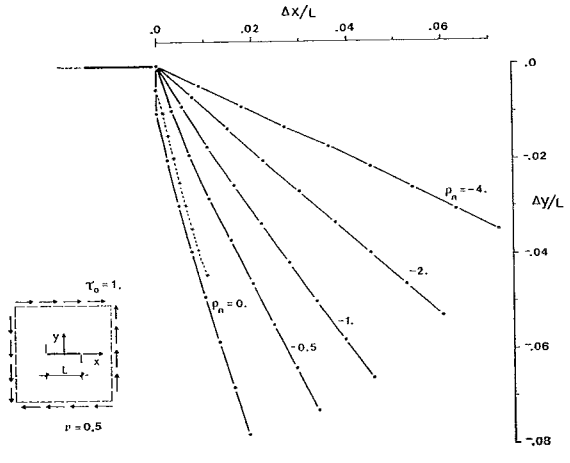

Fig. 14. - Propagation paths of a straight crack for uniform shear stress τ_0 at infinity and uniform internal pressure p_n. Other characteristics as in fig. 10.

Fig. 14. - Percorsi di propagazione di una frattura inizialmente rettilinea soggetta ad uno stato di sforzo tagliante τ_0 all'infinito ed a pressione interna p_n. Altre caratteristiche come in Fig. 10.

of the internal normal p_n and tangential p_t tractions. For these examples the internal loads follow the crack during its growth, i.e. both the initial crack and its propagation are subjected to the same internal load distribution. The numerical results clearly show the remarkable influence of the internal tractions on the fracture growth.

The results presented in fig. 13 refer to a straight crack, in an initially unstressed region, the propagation of which is caused by an internal shear traction distribution with value $p_t = 1$ on the initial crack and p'_t on the propagated part. Four analyses were performed, considering $p'_t = 0$ or $p_t' = p_t$ and $\Delta = 0.01L$ or $\Delta = 0.005L$. When $p'_t = 0$ the propagated crack has a relatively large radius of curvature and, as previously observed, the propagation path is practically independent from Δ. On the contrary, when $p'_t = p_t$ the radius of curvature decreases and, consequently, some influence of Δ on the path of growth is observed.

The last example (fig. 14) concerns the propagation of a fracture under uniform shear stresses at infinity, for various values of the internal pressure p_n. The influence of the length of the propagation increments is appreciable only when $p_n = 0$. In this case the numerical results indicate that the direction of initial propagation (90° from the main crack) is correctly determined, but that the lenght of the first increment is apparently overestimated by assuming $\Delta = 0.01L$ (solid line). In fact, if Δ is reduced to 0.005L, a propagation path (dashed line) almost parallel to the preceding one is obtained, the only appreciable difference being the lenght of the first increment.

Since all the performed analyses involve symmetric fracture propagations, the edge dislocations on one half of the crack only were considered as free variables. The entire initial crack was subdivided into 36 segments (thus leading to 36 free variables for the half-crack), and 10 new segments were added to each fracture tip at every propagation step. About 60 sec. of CPU time were required by an analysis with 9 increments (i.e. with 216 free variables for the last step), adopting Gauss-Jordan algorithm for system solution.

Alternative solution procedures, commonly used for boundary integral approaches and based on iterative algorithms, were not adopted here because of problems encountered in their application. These are related to the choice of the initial (trial) solution vector and to the convergency, which is not ensured for non positive definite matrix of coefficients.

5. Concluding remarks

A seemingly novel boundary integral approach has been presented for the propagation analysis of pressurized (or internally loaded) fractures in homogeneous, isotropic, elastic-brittle material. The problem is treated in plane strain or plane stress conditions and the crack is modelled with a distribution of edge dislocations seen as jumps in the components of the distortion vector as the crack contour is crossed in the direction normal to it.

The integral equations governing the problem are solved with a simple numerical technique, by discretizing the fracture into straight segments and assuming a constant distribution of edge dislocation within each segment.

The results of a series of analyses have been discussed concerning both the determination of stress distributions, stress intensity factors, etc. for non growing cracks, and the prediction of propagation paths for fractures subjected to various free field stresses and internal tractions.

The proposed approach appears to have some noticeable advantages with respect to other numerical procedures for fracture analysis because of the very limited amount of required geometrical data. In fact, all necessary information can be derived from the coordinates of the end points of the segments discretizing the crack. This allows to automatically generate the geometrical quantities describing the fracture growth with negligible computational and programming efforts.

The adopted technique for numerical solution presents the advantage of a very simple implementation. However, it requires relatively small subdivisions of the crack (with respect to other boundary integral approaches) in order to give reasonably accurate results. This is due to the crude assumption of piecewise constant distribution of edge dislocations along the crack, in general, and in the vicinity of the tips, in particular. With this respect, more sophisticated procedures for integration along the fracture (e.g. the one based on non-linear and singular « boundary elements » [BLANDFORD *et al.*, 1981]) should be tested and their performance compared (in terms of number of free variables necessary to obtain a predefined accuracy) with that of the adopted technique.

ACKNOWLEDGEMENTS

This study forms part of a research supported by the CNR (National (Italian) Research Council) under contract No. 80.00909.92, in the framework of a national research project on Geothermal Energy.

REFERENCES

BAZANT Z. P., CEDOLIN L., (1979) - *Blunt crack band propagation in finite element analysis.* J. Engng. Mechanics Div., ASCE, 105, EM2, pp. 297-315.

BLANDFORD G. E., INGRAFFEA A. R., LIGGET J. A. (1981) - *Two-dimensional stress intensity factor computations using the boundary element method.* Int. J. Numer. Methods Engng, vol. 17, pp. 387-404.

CEDOLIN L., BAZANT Z. P. (1980) - *Effect of finite element choice in blunt crack band analysis.* Comp. Meth. App. Mech. Engng. 24, pp. 305-316.

CHATTERJEE S. N. (1975) - *The stress field in the neighborhood of a branched crack in an infinite elastic sheet.* Int. J. Solids Structures, vol. 11, No. 5, pp. 521-538.

COTTEREL B., RICE J. R. (1980) - *Slightly curved or kinked cracks.* Int. J. of Fracture, vol. 16, No. 2, pp. 155-169.

INGRAFFEA A. R., HEUZE F. S. (1980) - *Finite element models for rock fracture mechanics.* Int. J. Anal. Numer. Methods Geomechanics, vol. 4, pp. 25-43.

JAWORSKI G. W., DUNCAN J. M., BOLTON SEED M. (1981) - *Laboratory study of hydraulic fracturing.* J. Geotechnical Engng. Div., ASCE, vol. 107, No. GT6, pp. 713-732.

MIR-MOHAMAD-SADEGH A., ALTIERO N. J. (1979) - *Solution of the problem of a crack in a finite plane region using an indirect boundary integral method.* Engng. Fract. Mech., vol. 11, pp. 831-837.

MURAKAMI Y. (1976) - *A simple procedure for the accurate determination of stress intensity factors by the finite element method.* Eng. Fract. Mech., vol. 8, p. 643.

MURAKAMI Y. (1980) - *Analysis of mixed-mode stress intensity factors by body force method.* Proc. 2nd Int. Conf. on Numerical Methods in Fracture Mechanics, Swansea, pp. 145-159.

MUSKHELISHVILI N. I. (1953) - *Some basic problems of the mathematical theory of elasticity.* P. Noordhoff Ltd, Groningen, Holland.

READ W. T. (1953) - *Dislocations in crystals.* McGraw Hill, New York.

RICE J. R., (1968) - *A path independent integral and the approximate analysis of strain concentration by notches and cracks.* Journal of Applied Mechanics, ASME, pp. 379-386.

SIH G. C. (1973) - *Some basic problems in fracture mechanics and new concepts.* Engineering Fracture Mechanics, vol. 5. pp. 365-377.

SOMMARIO

Un approccio per l'analisi della propagazione delle fratture nelle rocce

La ricerca di fonti alternative di energia ha recentemente portato allo sviluppo di nuove tecniche per l'estrazione di calore da rocce profonde di elevata temperatura che possono essere sintetizzate nei seguenti punti: due sondaggi verticali, opportunamente distanziati, vengono eseguiti sino alla profondità della roccia « calda »; una serie di fratture viene generata nella roccia, a partire dalle sezioni terminali dei sondaggi, per mezzo di un'elevata pressione idraulica. Le fratture congiungendosi creano un circuito ad U tra la superficie e la roccia profonda; ciò consente di pompare acqua a temperatura ambiente in uno dei sondaggi estraendo dal secondo acqua ad elevata temperatura, o vapore, che può essere usata per la produzione di energia elettrica.

È evidente che per un efficace impiego di questa tecnica è necessario poter predeterminare il percorso di propagazione delle fratture sulla base delle caratteristiche meccaniche della massa rocciosa, dello stato di sforzo in sito e della pressione applicata all'interno delle fratture stesse. Nel seguito vengono illustrate le caratteristiche di un approccio di calcolo per l'analisi della propagazione di fratture in pressione basato sul metodo degli integrali di contorno (Boundary Integral Method). Il problema è trattato in regime di deformazioni piane, assumendo che il mezzo contenente la frattura sia illimitato, omogeneo ed isotropo e che presenti un comportamento meccanico di tipo elastofragile. Caratteristica peculiare del metodo proposto è che i dati geometrici necessari si limitano a quelli descriventi la geometria della frattura. Ciò riduce sensibilmente la loro quantità, rispetto ad altri approcci numerici basati ad esempio sul metodo degli elementi finiti che richiedono anche la discretizzazione di una considerevole porzione del mezzo circostante la frattura, e consente un agevole aggiornamento dei dati geometrici durante il processo di propagazione. Nel seguito vengono anche presentati alcuni risultati ottenuti dalla soluzione di semplici esempi illustrativi.

Si consideri una frattura di forma generica e di lunghezza L situata in una regione piana indefinita (cf. Fig. 1) e si assuma che le superfici della frattura siano soggette a note distribuzioni di sforzi normali $p_n(s)$ e tangenziali $p_t(s)$, essendo s l'ascissa curvilinea lungo la frattura. Modellando la frattura come una distribuzione continua di Dislocazioni [READ, 1953] con componenti $C_n(s)$ e $C_t(s)$, gli sforzi $p_n(s)$ e $p_t(s)$ sono esprimibili tramite le eq. (1). Negli integrali di Cauchy (1a, b) le funzioni I_{ij} (s, $\bar{s}$) rappresentano la i-esima componente del vettore di sforzo in s causata da un valore unitario della j-esima componente del vettore delle dislocazioni in $\bar{s}$. Le espressioni di tali funzioni nel caso di comportamento elastico lineare, omogeneo ed isotropo sono riportate nelle eq. (2), (3) e (4).

Si noti che la presenza di uno stato di sforzo « naturale » nel mezzo circostante la frattura, in aggiunta a quello indotto dalla pressione interna alla frattura, può essere facilmente tenuto in conto tramite una semplice sovrapposizione degli effetti, come è schematicamente indicato in Fig. 2.

Per chiarire il significato fisico delle funzioni C_n e C_t si consideri che esse possono essere interpretate come discontinuità nelle componenti del vettore delle distorsioni attraverso il contorno della frattura nella direzione ad esso normale. Quindi in un punto $s=s_0$ assai prossimo alla punta s=o della frattura, assumendo che il tratto tra o ed s_0 sia assimilabile ad un segmento rettilineo, valgono le relazioni (7a, b) nelle quali Δu_n e Δu_t rappresentano le discontinuità delle componenti di spostamento normale e tangente al contorno della frattura.

Le relazioni (7) possono essere utilmente impiegate nel calcolo dei Fattori di Concentrazione degli sforzi K_I e K_{II}, tenendo conto che le eq. (11a, b) legano questi ultimi alle discontinuità delle componenti di spostamento. Eguagliando le espressioni delle discontinuità degli spostamenti (7) e (11) si ricavano le relazioni tra i fattori di concentrazione degli sforzi e le distribuzioni delle dislocazioni espresse dalle eq. (12).

Per risolvere le equazioni integrali (1a, b) può essere adottata una semplice tecnica numerica basata sulla suddivisione della frattura in N segmenti rettilinei (cf. Fig. 3) lungo i quali si assume valore costante delle dislocazioni. Le equazioni integrali vengono scritte per il punto centrale di ogni segmento, ottenendo così un sistema di 2N equazioni in 2N incognite rappresentate dai valori locali di C_n e C_t. Avendo risolto questo sistema è quindi possibile ricavare i fattori K_I e K_{II} tramite le

eq. (12a, b). Noti questi, ed adottando un opportuno criterio di propagazione, si può definire la direzione lungo la quale la frattura si estende per l'assegnata condizione di carico. La frattura viene estesa in tale direzione semplicemente aggiungendo alcuni segmenti a quelli già esistenti. Una nuova analisi può quindi essere eseguita per il successivo passo di propagazione.

La semplicità del metodo e l'esiguità dei dati geometrici necessari consente la sua implementazione in un semplice programma di calcolo che provvede automaticamente all'aggiornamento della geometria della frattura durante il processo di propagazione. Si deve tuttavia osservare che tale approccio soffre di alcuni inconvenienti. Infatti per poter determinare con ragionevole approssimazione i valori dei fattori di concentrazione degli sforzi è necessario suddividere la frattura in prossimità delle sue punte in segmenti di lunghezza particolarmente ridotta (dell'ordine di 1/1000 della lunghezza iniziale della frattura) e ciò ovviamente comporta un elevato numero di variabili libere nel sistema finale di equazioni, con conseguenti non trascurabili tempi di soluzione. Si deve poi tener conto che la lunghezza dell'incremento della frattura per ogni passo di propagazione deve essere scelta con attenzione, onde evitare che incrementi troppo lunghi portino a percorsi di propagazione dipendenti dal valore dell'incremento stesso.

I fattori di concentrazione degli sforzi ottenuti con l'approccio proposto per fratture a forma di arco circolare e per fratture contenenti un « gomito » sono presentati, rispettivamente, in Fig. 7 e 8. Le soluzioni numeriche rappresentate da punti, sono paragonate con quelle ottenute da altri autori [CHATTERJEE, 1975; COTTEREL, RICE, 1980], rappresentate da linee continue. Per migliorare l'approssimazione dei risultati relativi alla frattura contenente un gomito il programma di calcolo provvede a « raccordare » i due tratti rettilinei mediante un arco circolare. Tale arco è quindi suddiviso in segmenti rettilinei in modo tale da ridurre l'angolo tra due segmenti contigui al di sotto di circa 20°.

I risultati di alcune analisi di propagazione di fratture inizialmente rettilinee, di lunghezza L e soggette a varie condizioni di carico sono raccolti nelle Figg. 10, 11 e 14. Le analisi sono state condotte in regime di deformazioni piane, con modulo di deformabilità a taglio unitario ed adottando il criterio di Densità dell'Energia di Deformazione (Strain Energy Density Criterion) [SIH, 1973] per determinare la direzione di propagazione di ogni incremento della frattura. Tale criterio considera che la densità dell'energia di deformazione nelle vicinanze di una punta della frattura può essere espressa dall'eq. (20) dove W rappresenta l'energia di deformazione, V rappresenta il volume ed i coefficienti c_{ij} sono espressi dalle eq. (21) per problemi piani. Il criterio assume che la frattura si propaghi nella direzione θ caratterizzata dal valore minimo del fattore S di densità dell'energia (eq. 22a, b) e che la propagazione inizi quando il valore minimo di S raggiunge una soglia critica dipendente dal tipo di materiale. In Fig. 4 è rappresentato il sistema di coordinate r, θ utilizzato nella definizione del criterio di propagazione.

La fig. 10 mostra i percorsi di propagazione per fratture soggette ad uno stato di trazione monoassiale all'infinito, per valori del coefficiente di Poisson ν pari a 0.0 e a 0.5. Le linee a tratto pieno si riferiscono ad analisi nelle quali ogni incremento Δ della frattura è pari a 0.01 L, mentre per le linee tratteggiate $\Delta = 0.005$ L. Ogni incremento è a sua volta suddiviso in 10 segmenti rettilinei di uguale lunghezza. Per $\nu = 0.5$ si hanno percorsi di propagazione con raggio di curvatura relativamente grande che risultano praticamente indipendenti da Δ, mentre per $\nu = 0.0$ il raggio di curvatura diminuisce e l'influenza del valore di Δ sui risultati dell'analisi diviene sensibile. I risultati di Fig. 11 riguardano fratture soggette sia a trazione monoassiale all'infinito che a pressione interna. Per queste analisi, avendo assunto $\nu = 0.5$, l'influenza di Δ si è mostrata sempre trascurabile. Infine, in Fig. 14 vengono mostrati i percorsi di propagazione per fratture soggette ad uno stato di sforzo tagliante all'infinito e a pressione interna. L'influenza di Δ si avverte solo per il primo incremento nell'analisi con pressione interna p_n nulla, che avviene in accordo a quanto previsto dalla teoria in direzione normale a quella della frattura iniziale.

In base ai risultati ottenuti appare possibile concludere che l'approccio proposto è in grado di determinare con approssimazione sufficiente i valori dei fattori di concentrazione degli sforzi per fratture di diversa forma e che può determinare il percorso di propagazione di queste anche per processi di « crescita » non rettilinei. L'approccio mostra alcuni vantaggi rispetto ad altri metodi per l'analisi della propagazione di fratture, principalmente legati all'esiguità dei dati geometrici richiesti ed alla semplicità di implementazione dell'algoritmo. D'altro canto esso presenta alcuni inconvenienti che riguardano l'elevato numero di suddivisioni della frattura necessario per raggiungere una sufficiente approssimazione e la possibile influenza della lunghezza degli incrementi sui risultati dell'analisi. È ragionevole attendersi che una tecnica di integrazione più raffinata di quella qui adottata (ad esempio basata su andamenti di tipo lineare o parabolico delle dislocazioni lungo i segmenti discretizzanti la frattura) possa migliorare l'efficienza del metodo eliminando in buona parte gli inconvenienti denunciati.